Results in Materials 16 (2022) 100333

Contents lists available at ScienceDirect

Results in Materials

journal homepage: www.sciencedirect.com/journal/results-in-materials

Influence of accelerated weathering on the properties of flax reinforced PLA biocomposites

Moumita Sit [a], Jarren Ling [a], Chulin Jiang [c], Zhongyi Zhang [a], Moussa Khalfallah [b], Fanny Ioos [b], Erwan Grossmann [b], Hom Nath Dhakal [a,*]

[a] Advanced Polymers and Composites (APC) Research Group, School of Mechanical and Design Engineering, University of Portsmouth, Portsmouth, PO1 3DJ, UK
[b] Kairos, 1 Rue des senneurs, ZI du Moros, 29900, Concarneau, France
[c] Teesside University, School of Computing, Engineering and Digital Technologies, Middlesbrough, Tees Valley, TS1 3BX, UK

ARTICLE INFO

Keywords:
Biocomposites
Flax fibre
Accelerated weathering
Mechanical properties

ABSTRACT

The aim of the present study is to investigate the influence of accelerated weathering conditions (temperature and humidity) on the mechanical and physical properties of the flax fibre reinforced poly lactic acid (PLA) biocomposites. Two different types of biocomposites namely New Non-woven (NNW) and Conventional Non-woven (CNW) were developed for this study. After 500 h of exposure to humid environment with 95% relative humidity at 30 and 60 °C temperatures, the mechanical (tensile and flexural) and physical (surface roughness and hardness) behaviours were evaluated and compared with that of the dry specimens. Tensile and flexural properties were found to decrease significantly upon 500 h of exposure to accelerated weathering. The tensile strength of the biocomposite specimens exposed to 30 °C temperature and 95% RH demonstrated noteworthy improvement. Scanning electron microscopy (SEM) and X-ray micro CT images of fractured surfaces showed delamination, plasticization of matrix and fibre debonding due to exposure to various environmental conditions.

1. Introduction

Polymer composites are advanced materials that have been widespread in our daily lives and are regularly used in engineering applications. As the annual demand increase for polymer composites in the industry, it is not surprising that the yearly demand will experience a great increase over the next 20 years [1]. Due to most polymer composites being lightweight and sturdier than the other counterparts has enabled the use of it for automotive, aerospace, wind turbines, construction and more. However, the amount of wastage produced during the production stage has also greatly affected the environment [2]. With this concern of increase wastage, even recycling would be insufficient to mitigate this issue. Hence, the introduction of natural fibre composites (NFCs) would provide the aid in greatly addressing this issue with the benefits of recyclability, biodegradability and renewability, as well as a reduced cost in raw materials. Apart from being sustainable and biodegradable, NFCs offer several additional advantages lightweight, low density, high specific strength, low abrasiveness, CO_2 neutrality, among others in comparison to conventional glass fibres [3–10]. Many industrial sectors especially the automotive industry has witnessed a rapid increase in use of NFCs over the last decade in order to reduce the carbon footprint as well as the fuel consumption [11–15]. It has been observed from the available published literature that flax fibre has comparable specific properties to glass fibres [14,16,17]. However, these composite components are often exposed to variable temperature and moisture during their service life. The mechanical properties of fibre reinforced composites are very sensitive to environmental parameters like temperature change and moisture absorption. Continuous exposure to varying temperature and moisture levels may lead to the change in mechanical behaviour of the structural components. The exposure to temperature and moisture cause swelling or expansion of the polymeric matrix and reinforcements. Due to the degradation of material properties of hygrothermally affected composites, the stiffness and strength are altered considerably. Moreover, cyclic thermal and moisture loading further play role in deteriorating the performance of the composites leading to premature failure of the structures [18–20].

It has been recognised that natural plant fibres have some drawbacks including lower mechanical and thermal stability when compared to

* Corresponding author.
E-mail address: hom.dhakal@port.ac.uk (H.N. Dhakal).

https://doi.org/10.1016/j.rinma.2022.100333
Received 20 July 2022; Received in revised form 21 September 2022; Accepted 30 September 2022
Available online 13 October 2022
2590-048X/© 2022 The Authors. Published by Elsevier B.V. This is an open access article under the CC BY license (http://creativecommons.org/licenses/by/4.0/).

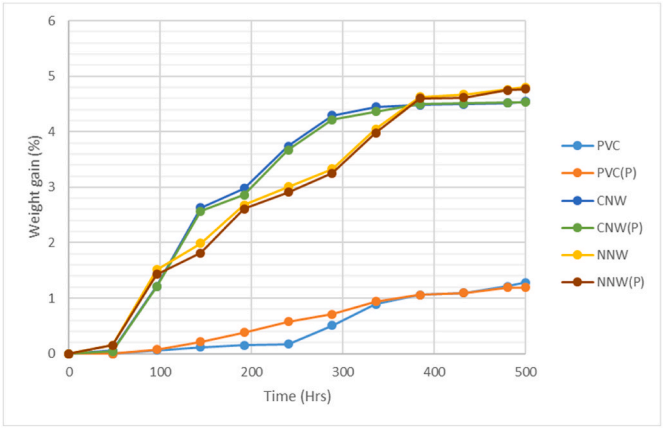

Fig. 1. Moisture absorption curve for different materials at 30 °C temperature and 95% RH (PVC: poly vinyl chloride; CNW: conventional non-woven, NNW: new non-woven; P represents printed).

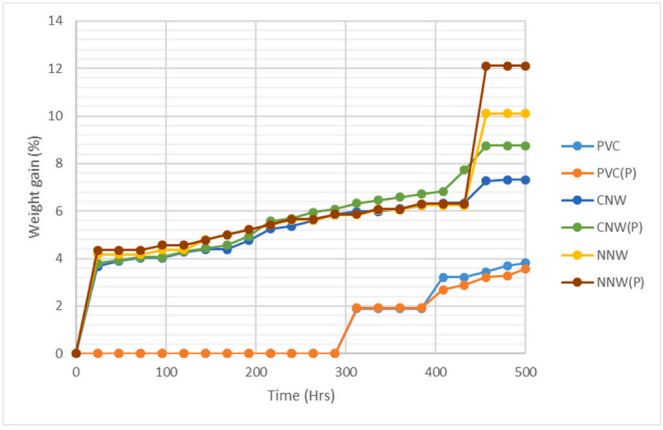

Fig. 2. Moisture absorption curves for different materials at 60 °C temperature and 95% RH (PVC: poly vinyl chloride; CNW: conventional non-woven, NNW: new non-woven; P represents printed).

synthetic fibres. The natural plant fibres absorb significant amount of moisture when exposed to atmospheric humid environments because of their hydrophilic nature and their chemical constituents. The presence of moisture causes swelling in natural fibres and their composites due to the existence of strong hydroxyl groups and other polar character of cellulose, hemicellulose, and lignin present in the fibres [21]. The swelling causes a continuous change of the structure of the fibre rendering a complex mechanism of moisture sorption in hydrophilic fibre materials [22]. Furthermore, the increase in moisture content causes significant loses of mechanical properties, dimensional instability and lowers the glass transition temperature of the polymeric matrix [4, 23–24,26], which in turn affect the overall performance of the composite structures. Many researchers [3,26–34] have investigated the effect of moisture exposure on the mechanical performance of NFCs. The effect of accelerated weathering has been reported by several researchers on kenaf/sisal fiber reinforced bio-epoxy composites [35], hemp fibre/polybenzoxazine composites [36], polylactic acid/agave fiber biocomposites [37], kenaf/pineapple-based composites [38], sisal/hemp fiber bio-epoxy based composites [39]. All of these studies have reported significant loses of mechanical properties with increase in moisture uptake as compared to the dry specimens. The reduction of the mechanical performance is mainly attributed to the swelling of natural fibres, delamination at the fibre-matrix interface and widening of the gap between the fibre bundles, under the effect of water absorption, which in turn affect the overall performance and the durability of composites [40].

The comprehensive review of the published literature indicates that although a lot of work have been reported on the environmental ageing

Table 1
Average tensile test results of dry samples; SD represents the standard deviation of the mean

Material	Mean Tensile Modulus (GPa) ± SD	Mean UTS (MPa) ± SD
CNW	5.67 (±0.51)	39.81 (±5.29)
NNW (Transverse)	4.82 ± 0.06	19.50 ± 2.93
NNW (Longitudinal)	8.15 ± 0.54	46.43 ± 4.00

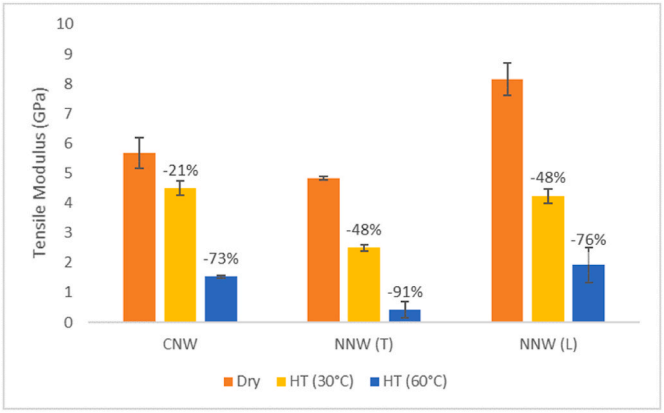

Fig. 4. Tensile modulus for different composites exposed to relative humidity of 95% RH at 30 °C and 60 °C.

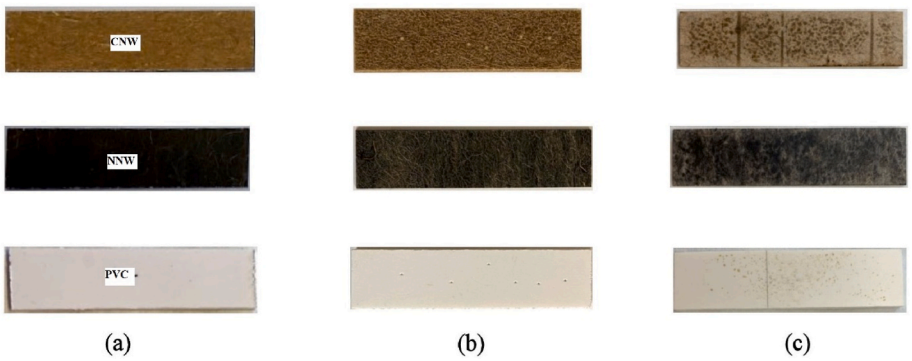

Fig. 3. Samples at different environmental conditions (a) before being exposed to humidity; (b) after 500 h of exposure to 95% RH at 30 °C; (c) after 500 h of humidity exposure to 95% RH at 60°.

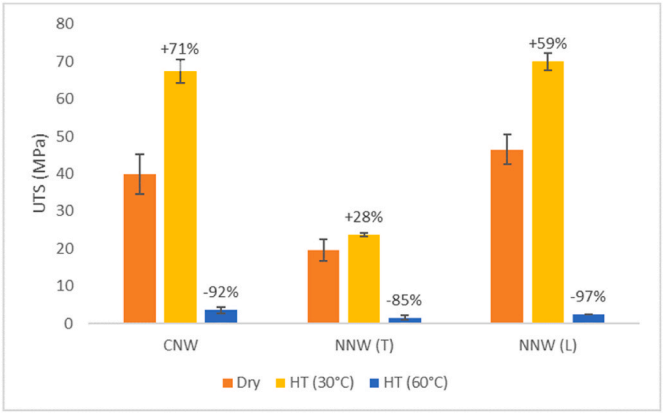

Fig. 5. Ultimate tensile strength for different composites exposed to relative humidity of 95% RH at 30 °C and 60 °C.

of natural fibre reinforced polymer composite, only limited articles are available on natural fibre reinforced PLA based biocomposites. In addition, the combined effect of moisture absorption, temperature and humidity on the mechanical properties of flax fibre reinforced fully biodegradable composite is not reported enough in the existing literature to the best of authors' knowledge.

The present study is aimed to design, develop and evaluate fully biodegradable composites, meeting some of the long-term durability requirements in point-of-purchase (POP) sectors. To achieve this goal, two types of biocomposites, composed of non-woven flax fibres and poly lactic acid (PLA), namely conventional non-woven (CNW) and new non-woven (NNW) are developed as sustainable fully green composites solution. The influence of accelerated weathering on the mechanical (tensile and flexural) and physical (surface roughness, and surface hardness) properties of these newly developed biocomposites are investigated. To replicate the real-life service conditions, the biocomposite samples were exposed to 95% RH at 30 and 60 °C temperature, respectively. The mechanical and physical properties have also been compared with those of conventional materials readily available in the market such as FOREX™, which is an expanded poly vinyl chloride (PVC) panel for indoor and outdoor use. The fractured surfaces after mechanical characterization have also been analysed to reveal the surface condition and possible failure mechanisms by using scanning electron microscopy (SEM) and X-ray micro CT.

2. Experimental

2.1. Materials

Three different types of materials have been used for the present study namely PVC, CNW (Conventional non-woven) and NNW (New non-woven). The newly developed composite material (produced and provided by Kairos, France) is a fully green composite with flax composite as reinforcement and PLA as matrix. The CNW was produced by using a needle punching process and the NNW was manufactured with a carding process offering improved control of the fibre orientation. The fibres of the NNW underwent a process through best selection and individualization. Consequently, the NNW does not contain any shive (less than 1%) whereas the CNW contain a significant amount of shives of around 10% compared to NNW.

- The CNW laminate is 2.7 mm thick and has the following layup:
- [PLA film of 435 g/m^2 + 7 layers of non-woven flax of 350 g/m^2 + PLA film of 435 g/m^2].
- The NNW laminate is 1.5 mm thick with the following layup:
- [PLA film of 435 g/m^2 + 6 layers of non-woven flax of 100 g/m^2 + PLA film of 435 g/m^2].

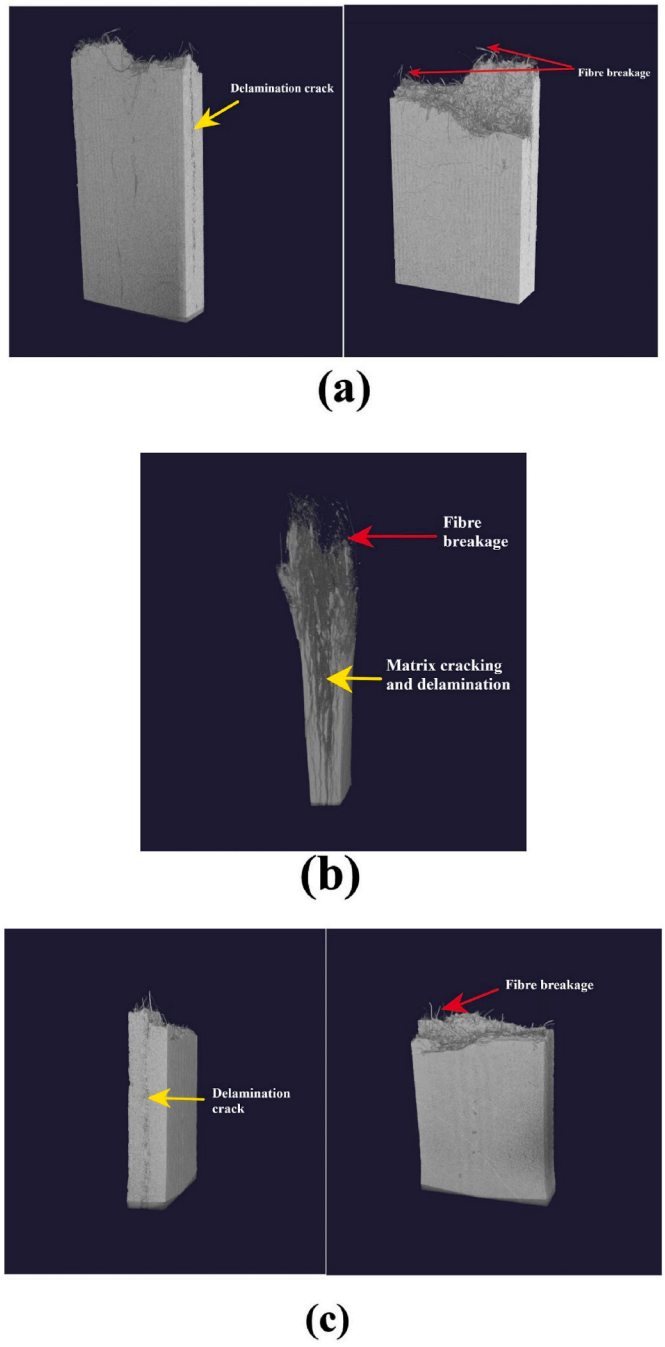

Fig. 6. X-ray μCT micrographs of the CNW samples depicting their fractured areas at different conditions (a) 30 °C, 95% RH; (b) 60 °C, 95% RH; (c) dry.

- The PVC sheets have thickness of 4.8 mm.

2.2. Fabrication of composite laminates

The non-woven flax/PLA laminates were prepared by compression moulding technique. In the step 1, PLA film PLA film 350 μm/2 layers of flax + PLA NW (350 g/m2) were stacked in symmetrically. In the step 2, The PLA film and flax/PLA were compressed at 190 °C for 5 min, under a pressure of 1 bar, and in step 3, the compressed laminates were consolidated. The detail steps of the fabrication process are provided in the authors' previous article [40].

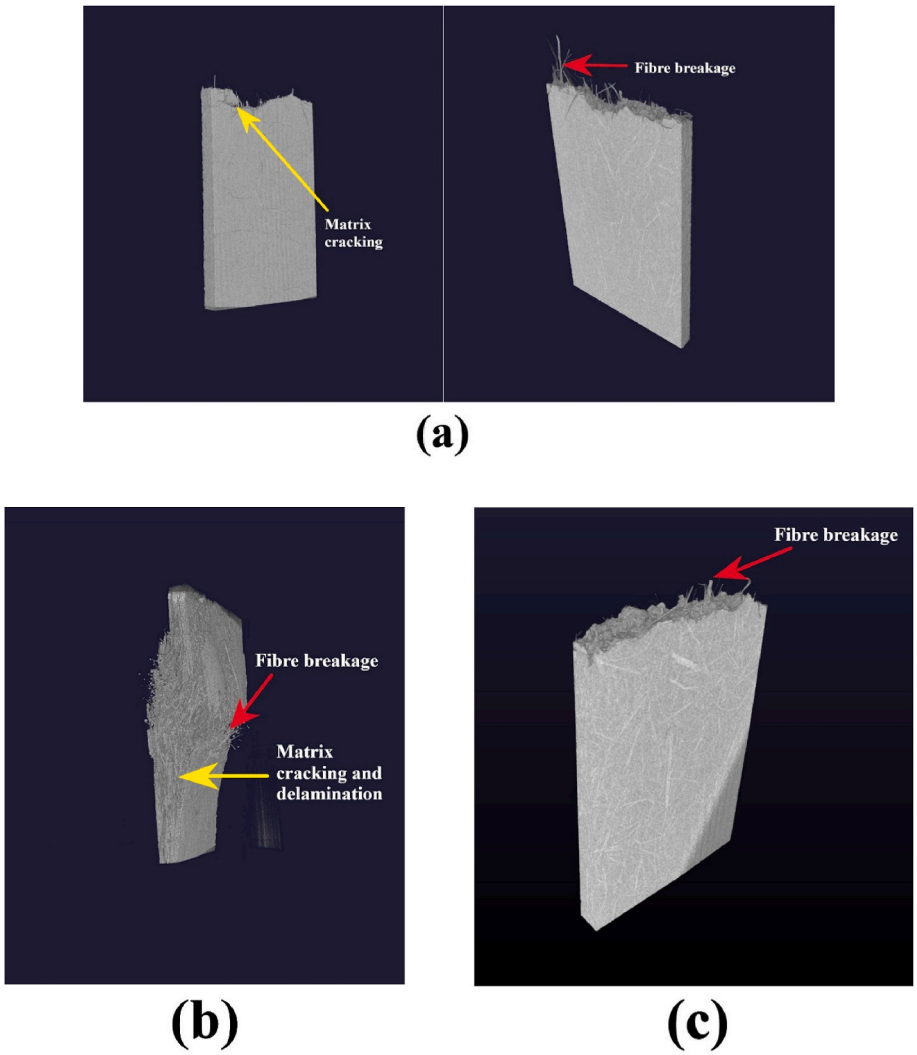

Fig. 7. X-ray μCT micrographs of the NNW longitudinal samples depicting their fractured areas at different conditions (a) 30 °C, 95% RH; (b) 60 °C, 95% RH; (c) dry.

2.3. Specimen preparation

All manufactured composite samples are cut in the dimension using a FB700 laser cutter by CadCam Technology and the PVC samples were cut with band saw cutter in accordance to the directive of British Standard EN ISO 527–2:1996 [41] for tensile tests and British Standard EN ISO 178:2010 [42] for flexural test. Samples were polished with a sand paper to obtain a good edge finish.

2.4. Accelerated weathering tests

Accelerated weathering of different biocomposite samples was carried out using TAS LTCL 350 environmental chamber. The samples were kept in an environmental chamber for two different exposure conditions (a) 60 °C temperature and 95% relative humidity (RH) and (b) 30 °C temperature and 95% RH. After every 24 h, the samples were removed from the chamber and weighed using an electronic balance (precision of 0.001 g). This process was repeated for 500 h for each exposure condition until the constant weight of all the samples were obtained. The visual observations and the measurement of surface roughness were also carried out at the interval of 48 h.

The percentage of the moisture absorption in the samples was calculated by the weight difference between the samples kept in the environmental chamber and the dry samples using theEquation (1).

$$\Delta M(t)(\%) = \frac{m_t - m_o}{m_o} \times 100 \quad (1)$$

where, $\Delta M(t)(\%)$ is moisture uptake at different time intervals (%), m_t is mass of the aged specimens at a specified time (t) and m_o is mass of the dry specimen.

2.5. Mechanical testing

2.5.1. Tensile and flexural testing

Tensile and flexural testing were performed on a Zwick/Roell Z030 universal machine using pull-to-break mode and bend-to-rupture modes, respectively. For the flexural testing, the test span was set at 50 mm (span-to-depth ratio of ~16) and crosshead speed of 2 mm/min. Flexural modulus and strength were calculated using the values obtained from force-displacement curves. The tests were conducted accordance with the standard for tensile characteristics [41] and the standard for flexural characteristics [42].

Tensile tests were performed at 2 mm/min crosshead speed; the tensile modulus, strength and strain to failure (STF) were determined by using the initial slope of the stress-strain curves obtained. The extensometer is set at the centre of the sample before the test starts and it is removed when the diagram program shows a read of 2% of the sample deformation. This procedure was done with all the samples. In order to investigate the effect of environmental ageing, at least 5 specimens from

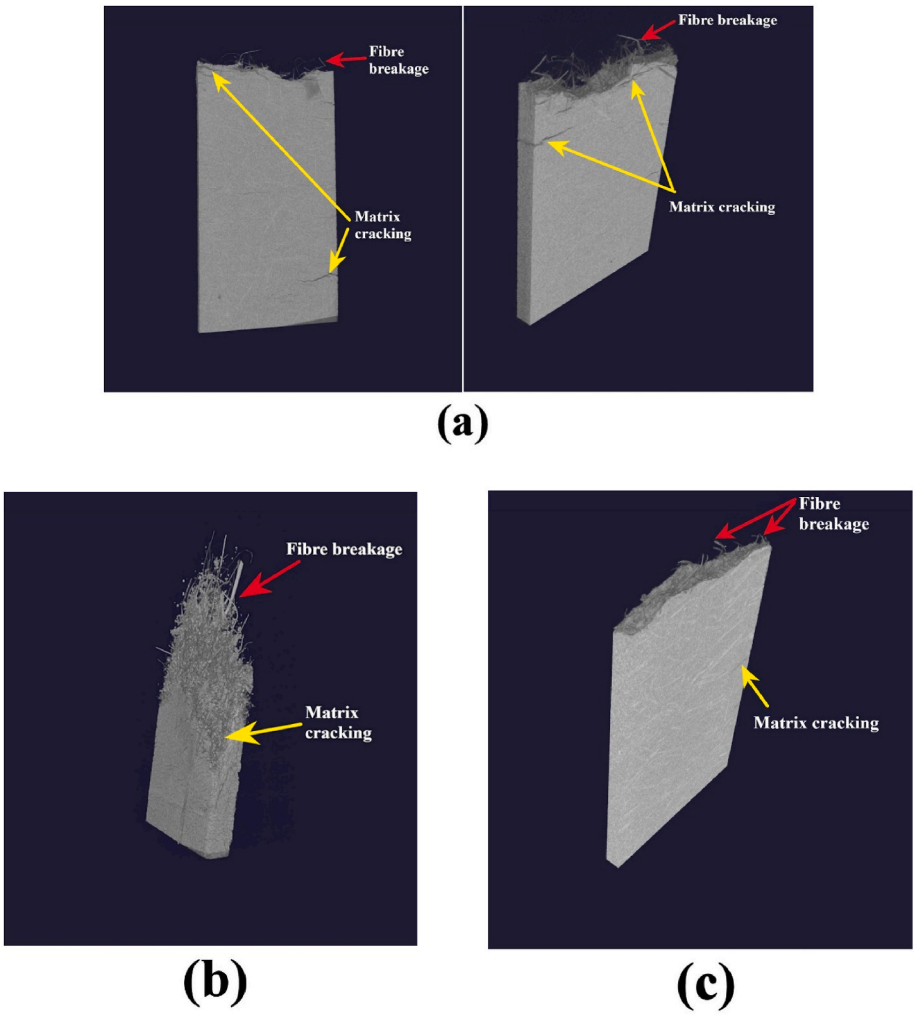

Fig. 8. X-ray μCT micrographs of the NNW transverse samples depicting their fractured areas at different conditions (a) 30 °C, 95% RH; (b) 60 °C, 95% RH; (c) dry.

each material at dry and aged conditions were tested and an average was taken. All tests were conducted at room temperature.

2.5.2. Surface roughness measurement

The surface roughness was measured using the Mitutoyo Surface Roughness Tester. This measurement was done to analyse the change in surface texture of the samples after undergoing weathering. The surface roughness has a crucial role in how the samples will interact with the environment. A rough surface usually has a higher rate of degrade when as compared to the smoother surface due to the higher friction produced. The parameter measured by the machine was Ra values. The value for Ra indicates the overall average surface roughness that could be detrimental to the overall properties of the samples.

2.5.3. Shore hardness measurement

The indentation hardness of a material can be determined by using the shore hardness method which uses a durometer that contains an indenter with a defined spring force. Each durometer has a different type from type A to D with a scale of 0–100. Depending on the material, a different type of durometer could be used as the hardness on the scale increases from 0 to 100. The shore hardness for each sample was measured by using shore D durometer.

Measurements were taken on different parts of the surface and an average was calculated.

3. Results and discussion

3.1. Moisture absorption behaviour

Figs. 1 and 2 depict the percentage of weight gain and moisture saturation against time for the different materials subjected to 95% relative humidity at 30 °C and 60 °C temperature respectively, before the mechanical testing. The moisture absorption behaviour has been studied for both printed and non-printed samples.

Based on the rate of moisture gain vs immersion time curves, the biocomposite samples (CNW and NNW) at 60 °C temperature started with a linear moisture uptake rate, and then rapidly increase for these samples. When it comes to absorbing moisture, saturation is reached for PVC samples after 432 h, and for CNW and NNW samples after 456 h. These weights increase percentages are around 3.81%, 8.76%, and 12.11%, respectively, for PVC, CNW, and NNW samples. Fibre cross-section and fibre morphology of natural plant fibres such as flax reinforced composites can contribute increased moisture diffusivity. The notable increased moisture uptake percentage for CNW and NNW is due to the presence of flax fibre in both materials, which is more susceptible to moisture due to the fibre cross-section and hollow lumen in the centre of the fibre morphology. Another factor contributing to high moisture absorption could be related to surface defects arising from manufacturing. The moisture ingress from the flax fibre surface can penetrate to the laminate creating water flow pathways as a result of degradation of flax composites surface due to the absorption of

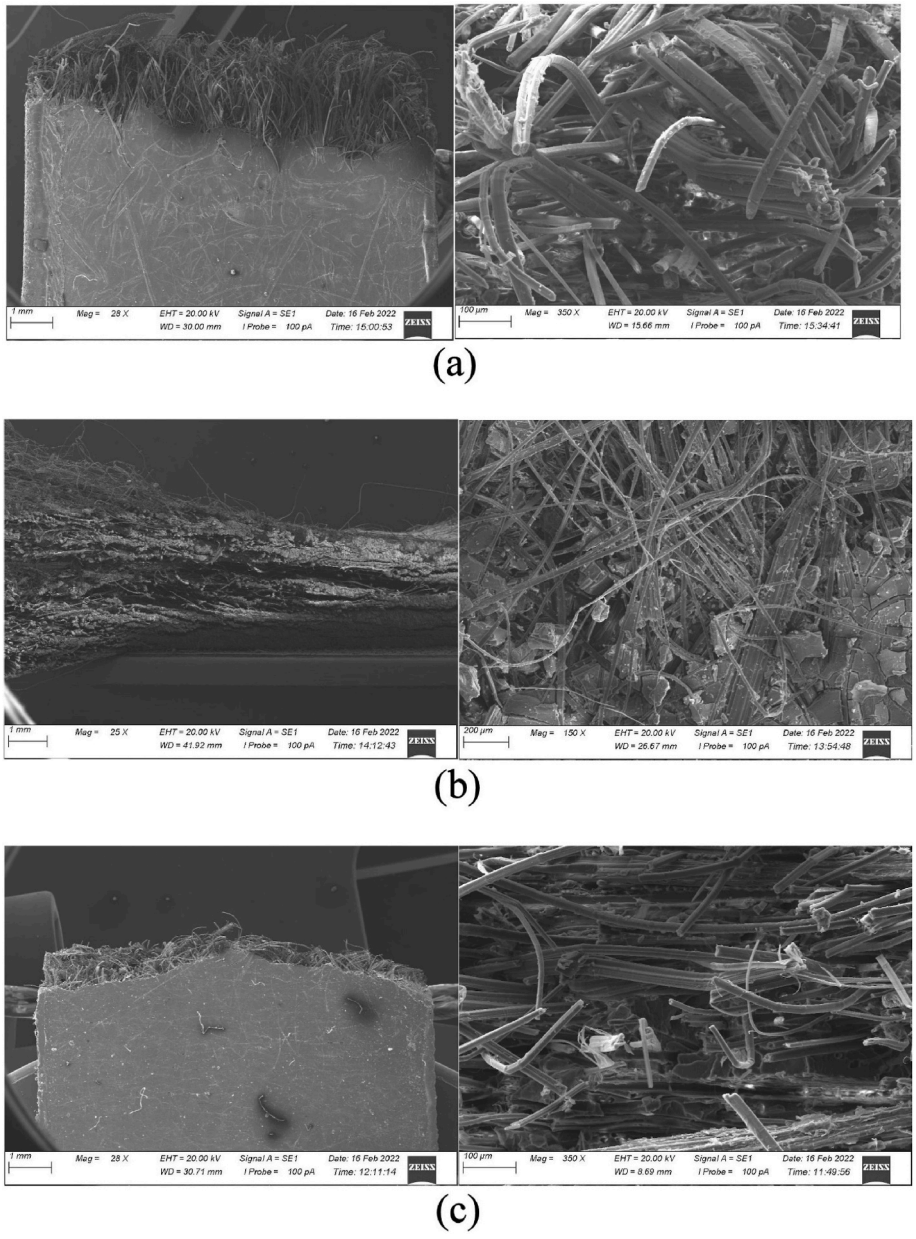

Fig. 9. SEM images of typical fracture section of the CNW samples depicting their fractured areas at different conditions (a) 30 °C, 95% RH; (b) 60 °C, 95% RH; (c) dry.

moisture. However, the scenario is different for 30 °C temperature.

It is clear from Fig. 1 that the rate of moisture absorption is somewhat consistent for the biocomposite samples until the saturation point. Unlike 60 °C temperature, the saturation at 30 °C temperature is attained quite earlier for the biocomposite samples, amounting to be 336 h for CNW and 384 h for NNW. The moisture gain percentages of PVC, CNW and NNW at 30 °C are around 1.2%, 4.5% and 4.8% respectively.

Fig. 3(a) depicts the visual appearance of the samples before putting into the environmental chamber while Fig. 3(b) and (c) depict the visual appearance of the samples after moisture degradation at 30 °C and 60 °C temperature, respectively.

Biocomposite samples exposed to accelerated weathering (60 °C temperature and 95% RH) experienced a significant amount of degradation including colour change and blistering of the surface. Whereas for PVC samples, minute changes were observed like pigmentation on the surface. However, no substantial changes were observed in the samples exposed to 30 °C temperature and 95% relative humidity except moist surfaces of the CNW and NNW samples.

3.2. *Effect of accelerated weathering on tensile properties*

The Young's modulus and tensile strength of different samples in dry condition are summarised in Table 1. As expected, it can be seen that the NNW in transverse fibre direction has the lowest tensile strength and modulus. The tensile modulus and the ultimate tensile strength (UTS) of the test samples are presented in Figs. 4 and 5 for different exposure condition. It is evident from Figs. 4 and 5 that the tensile modulus and strength of the samples degrades significantly with accelerated weathering. Because of their hydrophilic nature, the natural fibres are susceptible to moisture absorption which in turn causes swelling of the fibres as well as the expansion of the matrix and weakens the fibre matrix interface. This increases the amount of unfavourable influence on the tensile characteristics.

In dry condition, the NNW longitudinal sample has the highest

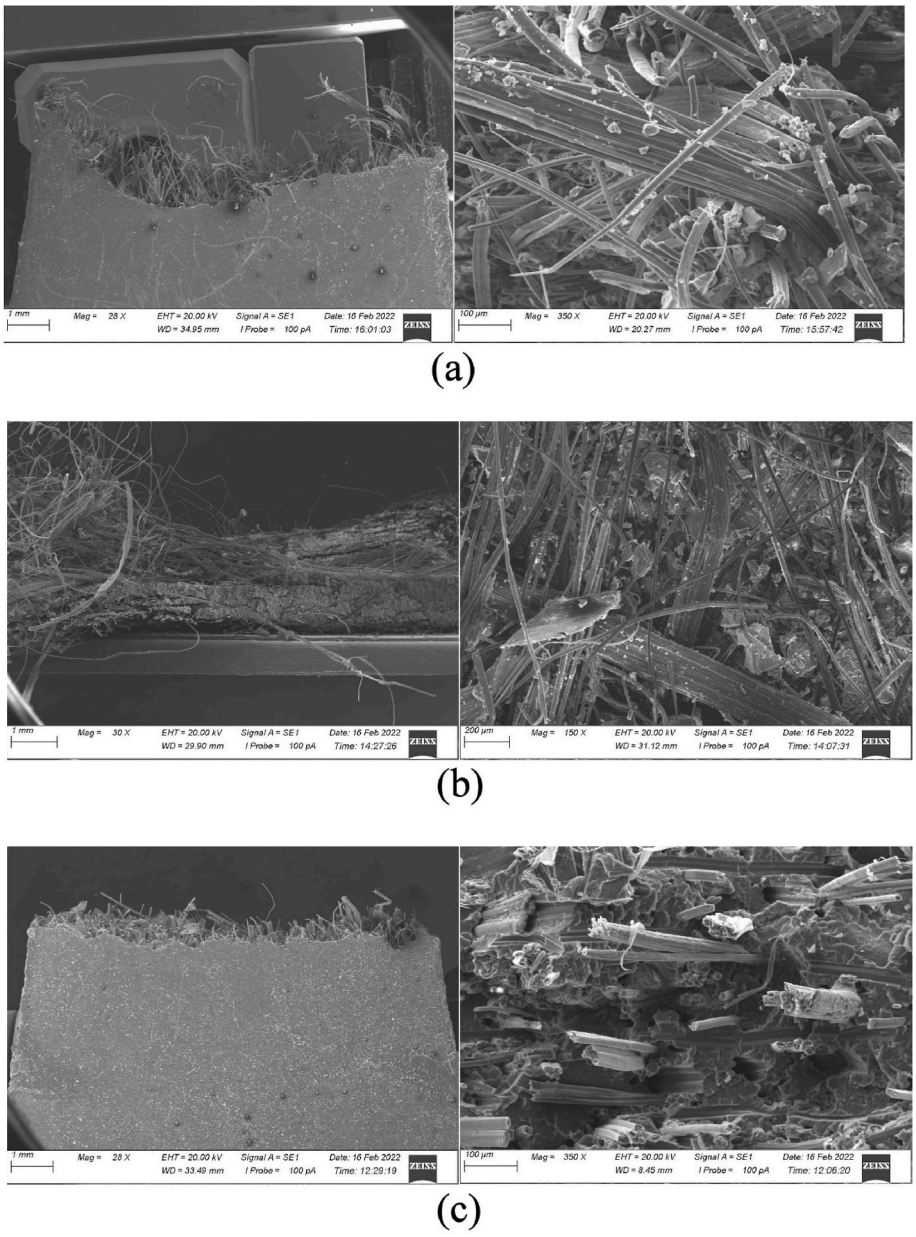

Fig. 10. SEM images of typical fracture section of the NNW longitudinal samples depicting their fractured areas at different conditions (a) 30 °C, 95% RH; (b) 60 °C, 95% RH; (c) dry.

Young's modulus of 8.15 GPa followed by CNW and the NNW transverse sample has the weakest modulus of 4.82 GPa. The higher modulus of the NNW longitudinal sample can be attributed to the architecture and controlled fibre direction of the NNW. The carding technology offers improved ability to control the fibre direction in the NNW compared to the needle punching process used for the CNW.

After exposure to the harsh humid environment (60 °C and 95% RH), the tensile modulus and strength deceases by approximately 73% and 93%, respectively in the case of CNW. For NNW, with moisture exposure, the tensile modulus and strength was decreased approximately by 91% and 97% percent, respectively for transverse direction. However, for longitudinal direction, with exposure to moisture, the modulus and strength were decreased by approximately 76% and 91%, respectively. The cause of this behaviour might be ascribed mainly to the plasticization of the PLA reaching its glass transition temperature (50–80 °C), which led to de-bonding of the fibres and loss of structural integrity and consequently exposing the fibres to moisture attack. The penetration of water molecules into the fibre–matrix region led to the change of dimensions of the composite specimens and caused weak interfacial bonding, thereby decreasing the tensile properties. Dimensional variation occurred due to the swelling of the fibre, which led to fibre detachment from the matrix, creating damaged fibre matrix bonding. The significant reduction in mechanical performance due to moisture absorption is related to plastization, debonding in the fibre-matrix interface due to swelling stress. The damaged interface further contributed to the failure of the composite laminate.

However, after exposure to mild humid environment (30 °C temperature and 95% RH), the materials behave significantly different in terms of tensile strength than that of the dry one. It is observed from Fig. 5 that the tensile strength of the humid CNW sample is increased by 71% than that of the dry CNW samples. Similar trend is observed for the NNW samples with an increment of 59% and 28% of tensile strength in longitudinal and transverse direction, respectively. Although the tensile modulus for the same environmental exposure is decreased by

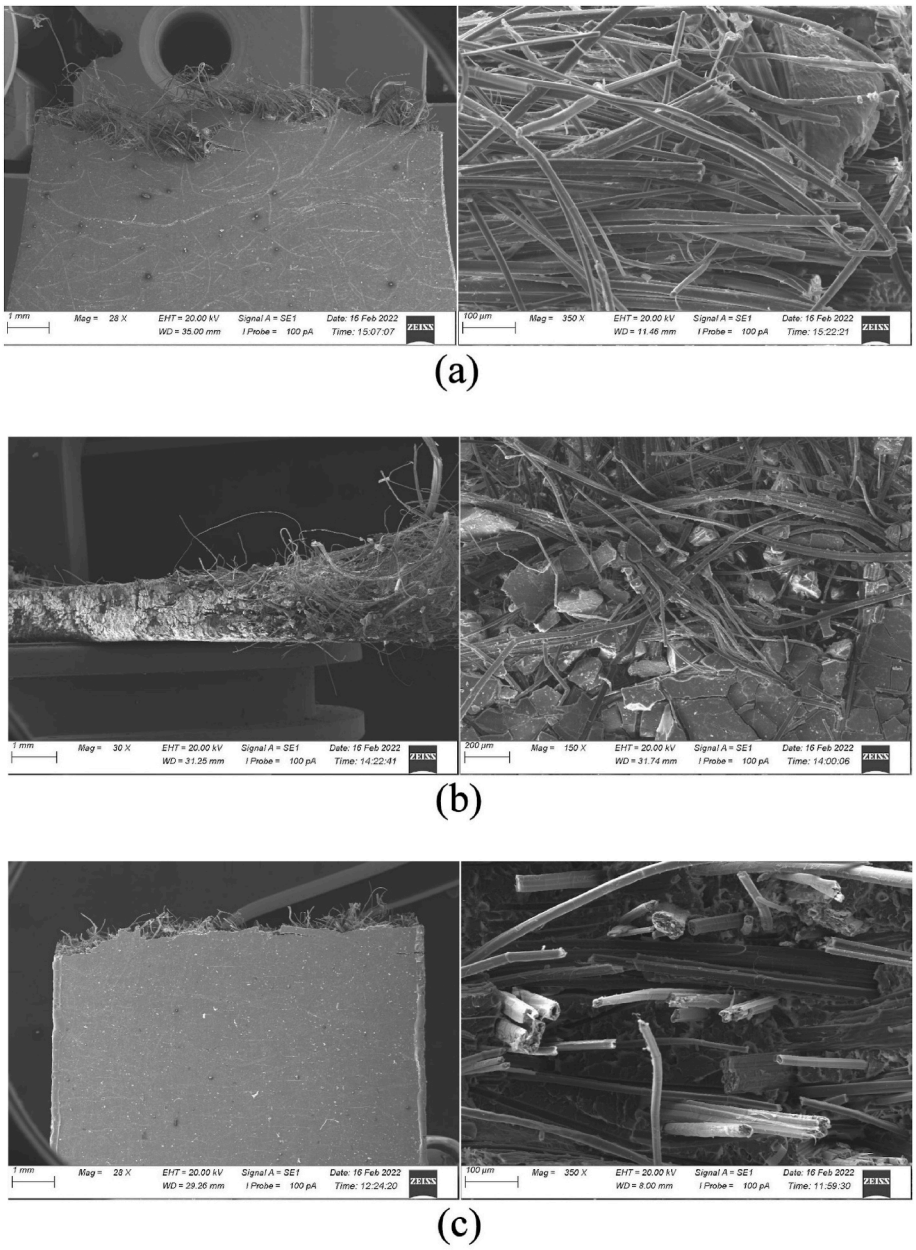

Fig. 11. SEM images of typical fracture section of the NNW longitudinal samples depicting their fractured areas at different conditions (a) 30 °C, 95% RH; (b) 60 °C, 95% RH; (c) dry.

approximately 21%, 48% and 48% for CNW, NNW longitudinal and NNW transverse samples respectively. The increment of the tensile strength may be attributed to the high amount of water absorption that resulted in swelling of the fibres. The swelling of the fibres is further able to fill up the gaps between the fibres and the polymeric matrix that may occur during the manufacturing process and subsequently can lead to the improvement in tensile strength of the composites. Similar phenomena have been observed for flax fibre reinforced bioepoxy composites after 768 h of water immersion [43]. The similar effect has been reported for jute fibre reinforced polypropylene [44] and hemp fibre reinforced unsaturated polyester composites with a fibre volume fraction of 0.26 [30] after a period of water immersion.

X-ray computed micro-tomography (μ-CT) scans and scanning electron microscopy (SEM) were conducted around the fractured areas of each material. The μ-CT scans were performed in order to establish a better understanding of the damage mechanisms in each material after being exposed to different environmental condition and the damaged surface for each specimen are shown in Figs. 6–8.

It is evident from the μ-CT scans that the damage mechanisms mainly include fibre breakage, fibre pull out and matrix cracking. Delamination also appears to be present in some cases. It can be observed from the fractured surface that the failure of the dry specimens exhibits brittle behaviour whereas the failure at 60 °C and 95% RH is ductile in nature owing to the plasticization of the matrix. It is also interesting to note that the fractured surface at dry condition for each material appears to be even and uniform with fewer fibre breakages whereas extensive fibre breakage, matrix cracking and uneven fractured surface can be seen for the same materials after exposure at 30 °C temperature and 95% RH.

This difference in fracture mechanism also demonstrates the improvement of the tensile strength in these composite laminates after being exposed at 30 °C temperature and 95% RH compared to dry condition. However, the damage mechanism in the samples after exposure at 60 °C temperature and 95% RH is significantly different to other two conditions, due to the harsh environment. The failure is

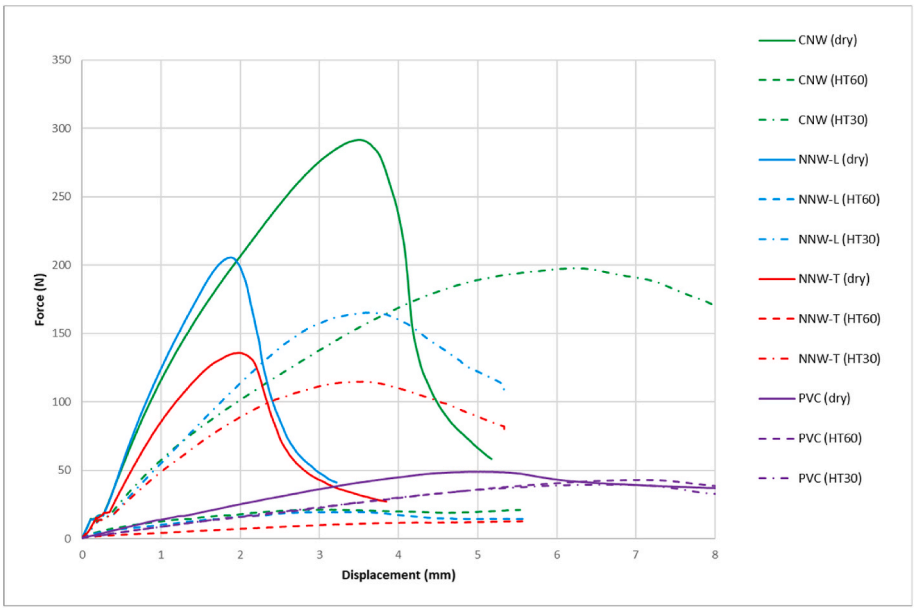

Fig. 12. Force-displacement curves obtained from 3-point bending test for different samples at different environmental conditions (HT represents elevated temperature at 95% RH).

Table 2
Average flexural test results of dry samples; SD represents the standard deviation of the mean.

Material	Flexural modulus (GPa) ± SD	Flexural strength (MPa) ± SD
CNW	5.90 ± 1.46	112.35 ± 15.13
NNW (Longitudinal)	6.86 ± 0.93	133.98 ± 14.37
NNW (Transverse)	4.76 ± 0.22	84.81 ± 2.25
PVC	1.38 ± 0.05	23.9 ± 0.23

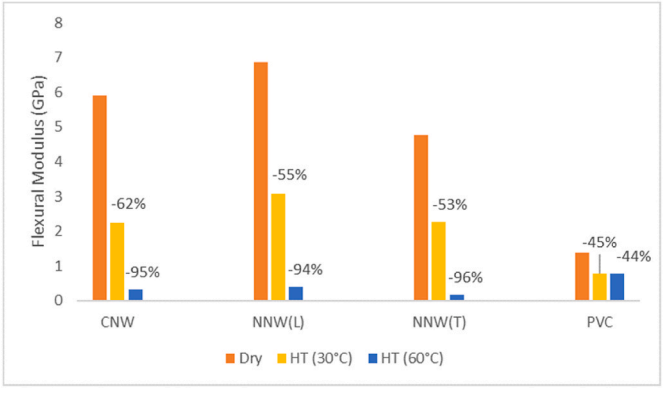

Fig. 13. Flexural modulus for different materials exposed to relative humidity of 95% RH at 30 °C and 60 °C.

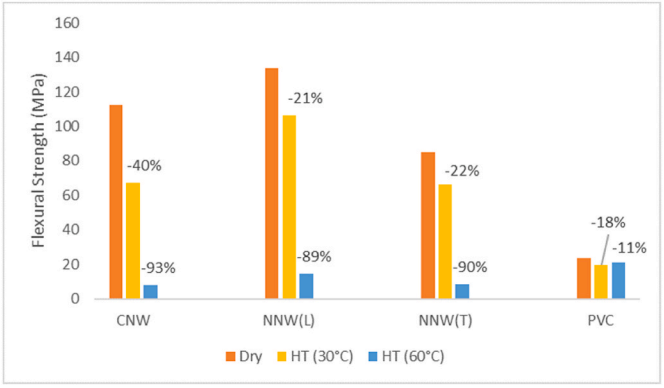

Fig. 14. Flexural strength for different materials exposed to relative humidity of 95% RH at 30 °C and 60 °C.

Table 3
Average surface roughness (Ra) values of dry samples; SD represents the standard deviation of the mean.

Material	Average Ra (μm)	SD (μm)
CNW	0.747	0.111
NNW	0.631	0.058
PVC	1.927	0.096

mainly caused by the matrix cracking, fibre-matrix debonding and delamination. Due to the exposure in harsh environment, the PLA reached its glass transition temperature of leading to plasticization and loss in strength of the matrix material.

These observations were confirmed by the SEM images of the fractured samples as shown in Figs. 9–11. The SEM images in Fig. 9(c) and (a) show the fractured surface of the CNW specimen at dry condition and exposure at 30 °C and 95% RH respectively. These SEM images also exhibit the fibre swelling and enhanced bonding between the fibres and the matrix after exposure to humid condition compared to the dry condition, which indicates a more efficient transfer of stress along the fibre-matrix interface before the failure of the composite. Additionally, the fractured surface of the dry specimens shows fibre breakage in a more brittle manner, compared to the fractured surface of the specimens exposed to 30 °C and 95% RH. This phenomenon in turn justifies the improvement of tensile strength of the 30 °C humidity specimens compared to the dry specimen. The plasticization and the loss of structural integrity of the matrix material after exposure at 60 °C and 95% RH is evident from Fig. 9(b). Similar effect and fracture surface were also observed for NNW longitudinal and transverse samples as presented in Figs. 10 and 11.

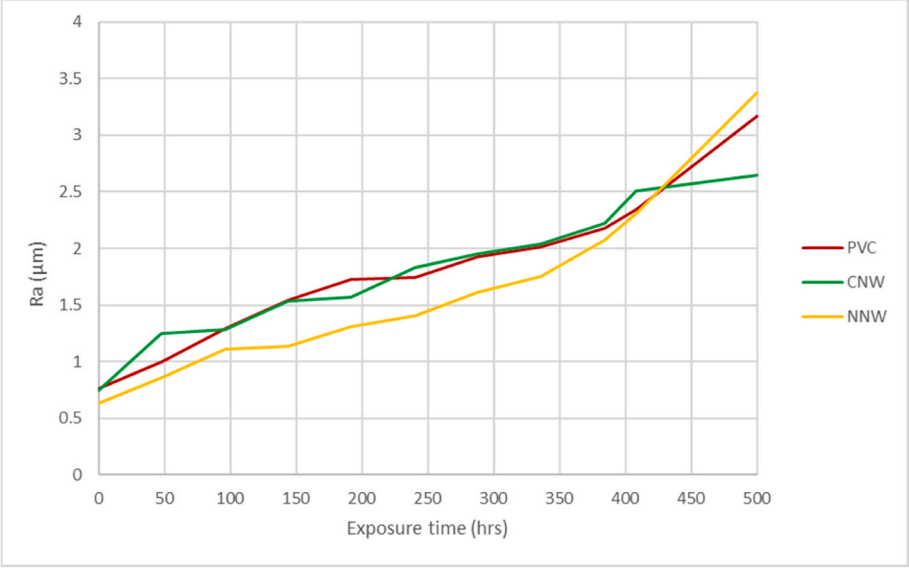

Fig. 15. Surface roughness (Ra) measurement of the humidity samples (60 °C temperature and 95% RH) at different time intervals.

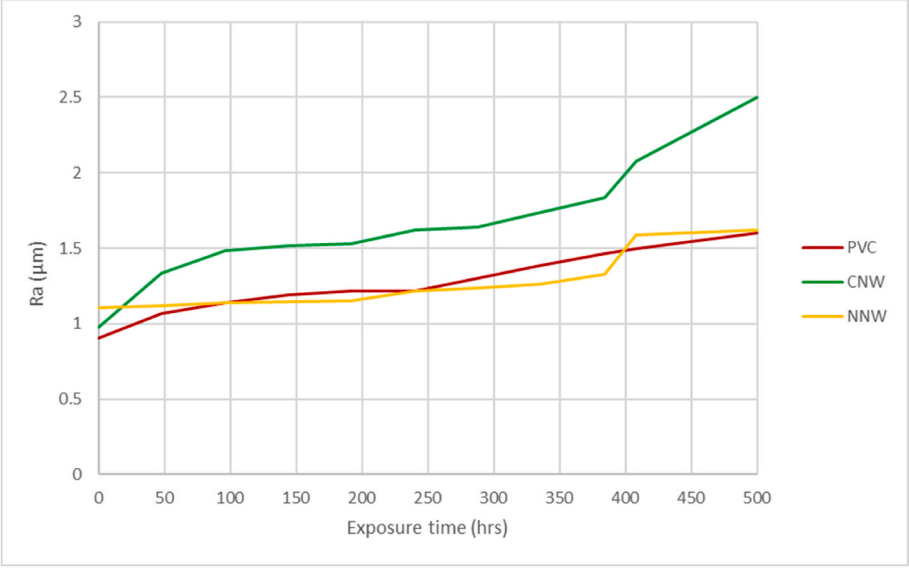

Fig. 16. Surface roughness (Ra) measurement of different samples at 30 °C temperature and 95% RH at different time intervals.

Table 4
Values of Shore D hardness for different materials in different environmental conditions.

Material	Dry Samples	Humidity Samples (95% RH at60 °C)	Humidity Samples (95% RH at30 °C)
PVC	37.0 ± 1.4	38.2 ± 1.3	37.6 ± 1.5
CNW	85.0 ± 0.7	67.0 ± 1.2	79.4 ± 0.5
NNW	85.6 ± 0.9	63.8 ± 1.8	79.6 ± 0.5

3.3. Effect of accelerated weathering on flexural properties

The flexural behaviour of the samples is represented in the form of force-displacement curves obtained from the 3-point bending tests. Typical load versus displacement traces were depicted in Fig. 12. It can be observed from Fig. 12 that the dry samples displayed a steep gradient for CNW and NNW which indicated a more brittle fracture. While the humid samples displayed a flatter gradient, indicating the sign of ductile fracture.

The average flexural strength and modulus of the test samples for different environmental conditions calculated employing standard formula using load against displacement curves. The flexural strength and modulus of the dry samples are presented in Table 2. The change in flexural modulus and flexural strength of the test samples for different environmental conditions are depicted in Figs. 13 and 14.

It can be observed from Table 2 that the NNW specimens at dry condition in longitudinal fibre direction has the highest flexural modulus and flexural strength of 6.86 GPa and 133.98 MPa respectively. It is evident from Figs. 13 and 14 that the strength and modulus were decreased significantly for CNW and NNW with exposure to humid environment. For the CNW sample, for example, at exposure at 95% RH, 60 °C, the strength was recorded at 7.96 MPa (a decrease of 93%) and modulus of 0.31 GPa, (a decrease of 95%), respectively. However, this is not the case for PVC samples. The decrease in flexural modulus and flexural strength of PVC in wet condition is recorded as 43% and 11% respectively.

Exposure to 95% RH at 30 °C temperature renders similar effect on the flexural properties of the composite samples. However, the reduction in flexural modulus and flexural strength is much lesser compared to the exposure of 95% RH at 60 °C. The flexural modulus and the flexural strength of the CNW was found to be 67.09 MPa and 2.24 GPa respectively, which is 62% and 40% lower than the dry samples respectively. The reduction in the flexural strength can be attributed to the swelling of the fibres as a result of the penetration of water molecules in the interfacial region between the fibre and the matrix. Due to this, gaps formed between the fibre and the matrix, which in-turn led to the debonding of the fibre from the matrix. The presence of moisture in the fibre degrades them, separating the fibres into fibrils. It may also be caused by the weak interfacial adhesion between fibre and matrix, as a result of the appearance of hydrogen chemical bonds between the cellulose fibre (flax fibres) and the water molecules. When water molecules penetrated the macro-voids and free space of the matrix, new cavities and cracks formed, acting as a water transport pathway within the composites and reducing interfacial bonding.

4.4. Effect of accelerated weathering on surface roughness

The average surface roughness (Ra) values of the dry samples are presented in Table 3. The change in roughness parameters after the exposure to 95% RH at 60 °C and 30 °C temperature is shown in Figs. 15 and 16 respectively. It can be seen from Fig. 15 that the relative humidity at 60 °C temperature effects all the parameters of surface roughness in all materials. It was noted that as time goes by in humid condition, the value of Ra increased for all the samples. Increasing exposure time brings about an increase in weight gain, which in turn causes an increase in surface roughness. Hence, it was apparent that the increase in relative humidity adversely influenced the overall surface quality of the samples. Similar trend is observed for the humidity samples at 30 °C temperature (Fig. 16) with lesser variation.

4.5. Effect of accelerated weathering on shore hardness

The values for shore hardness measured on a Shore D durometer on different samples were tabulated in Table 4. It was observed from the table that the hardness of both CNW and NNW were adversely affected by the humid condition at 60 °C temperature with a significant decrease of approximately 21% and 25% respectively. Whereas the exposure to 30 °C temperature and 95% RH has less significant effect on the hardness of the biocomposites. The hardness is reduced by approximately 6.58% and 7% for CNW and NNW respectively. However, the PVC samples had little effect from being exposed to humid environment. The reduction in hardness of the composite specimens, when exposed to humid environment, also supports the ductile nature of the failure after tensile test.

5. Conclusions

Flax fibre reinforced PLA biocomposites were exposed to accelerated weathering conditions for a prolonged time period to study the influence on the mechanical and physical properties. The flexural and the physical properties of the biocomposites are compared with those of PVC as reference material. The samples were exposed to 95% RH at 30° and 60 °C temperature. The study shows that the water absorption increases significantly at higher temperature. It is found that the mechanical and the physical properties of the biocomposites are significantly better than that of the PVC. Exposure to humidity at higher temperature results in significant reduction in the tensile properties due to the plasticization of the matrix material. However, the tensile strength of the biocomposites increase considerably after exposure to humidity at 30 °C compared to the dry specimens. The results indicate that swelling of flax fibres in the composite material caused due to moisture absorption can have positive effects on the tensile strength. The μ-CT and SEM images illustrate that the damage mechanism mainly include fibre breakage, fibre pull out and matrix cracking whereas plasticization of the matrix can be observed for the biocomposite samples exposed to 60 °C temperature. Flexural properties decrease with the increase in moisture absorption content. Tensile modulus was found to decrease with moisture absorption as a sensitive property of the fibre. The swelling of the fibres and the plasticization of the matrix also result in lower hardness and increased surface roughness of the materials exposed to humid environment. Based on the results obtained, it may be concluded that the flax fibre reinforced PLA composites can be used as a potential substitute of PVC for the use in POP sectors to achieve environment friendly and economic design.

Credit author statement

All persons who meet authorship criteria are listed as authors, and all authors certify that they have participated equally in the work to take public responsibility for the content, including participation in the concept, design, analysis, writing, or revision of the manuscript.

Funding

This research was funded by the INTEREG VA Program, FLOWER project, Grant Number 23

Declaration of competing interest

The authors declare that they have no known competing financial interests or personal relationships that could have appeared to influence the work reported in this paper.

[25]

Data availability

The authors do not have permission to share data.

References

[1] D.E. MacArthur, D. Waughray, M.R. Stuchtey, The new plastics economy, rethinking the future of plastics, World Economic Forum, 2016.
[2] D. Ayre, Technology advancing polymers and polymer composites towards sustainability: A review, Curr. Opin. Green Sustain. Chem 13 (2018) 108–112, https://doi.org/10.1016/j.cogsc.2018.06.018.
[3] D. Scida, M. Assarar, C.R. Poilâne, R. Ayad, Influence of hygrothermal ageing on the damage mechanisms of flax-fibre reinforced epoxy composite, Compos. B Eng. 48 (2013) 51–58, https://doi.org/10.1016/j.compositesb.2012.12.010.
[4] M. Berges, R. Léger, V. Placet, V. Person, S. Corn, X. Gabrion, J. Rousseau, E. Ramasso, P. Ienny, S. Fontaine, Influence of moisture uptake on the static, cyclic and dynamic behaviour of unidirectional flax fibre-reinforced epoxy laminates, Compos. Appl. Sci. Manuf. 88 (2016) 165–177, https://doi.org/10.1016/j.compositesa.2016.05.029.
[5] L. Yan, N. Chouw, K. Jayaraman, Flax fibre and its composites – A review, Compos. B Eng. 56 (2014) 296–317, https://doi.org/10.1016/j.compositesb.2013.08.014.
[6] B. Szolnoki, K. Bocz, P.L. Sóti, B. Bodzay, E. Zimonyi, A. Toldy, B. Morlin, K. Bujnowicz, M. Wladyka-Przybylak, G. Marosi, Development of natural fibre reinforced flame retarded epoxy resin composites, Polym. Degrad. Stabil. 119 (2015) 68–76, https://doi.org/10.1016/j.polymdegradstab.2015.04.028.
[7] K.L. Pickering, M.G.A. Efendy, T.M. Le, A review of recent developments in natural fibre composites and their mechanical performance, Compos Part A Appl Sci Manuf 83 (2016) 98–112, https://doi.org/10.1016/j.compositesa.2015.08.038.
[8] M. Habibi, L. Laperrière, H. Mahi Hassanabadi, Replacing stitching and weaving in natural fiber reinforcement manufacturing, part 1: mechanical behavior of unidirectional flax fiber composites, J. Nat. Fibers 16 (7) (2018) 1064–1076, https://doi.org/10.1080/15440478.2018.1448321.
[9] M. Habibi, L. Laperrière, H. Mahi Hassanabadi, Replacing stitching and weaving in natural fiber reinforcement manufacturing, part 2: mechanical behavior of flax fiber composite laminates, J. Nat. Fibers 7 (3) (2018) 388–397, https://doi.org/10.1080/15440478.2018.1494079.
[10] R. Siakeng, M. Jawaid, M. Asim, S. Siengchin, Accelerated weathering and soil burial effect on biodegradability, colour and textureof coir/pineapple leaf fibres/PLA biocomposites, Polymers 12 (2) (2020) 458, https://doi.org/10.3390/polym12020458.
[11] F.M. AL-Oqla, S.M. Sapuan, Natural fiber reinforced polymer composites in industrial applications: feasibility of date palm fibers for sustainable automotive

industry, J. Clean. Prod. 66 (2014) 347–354, https://doi.org/10.1016/j.jclepro.2013.10.050.
[12] C. Alves, P.M.C. Ferrão, A.J. Silva, L.G. Reis, M. Freitas, L.B. Rodrigues, D.E. Alves, Ecodesign of automotive components making use of natural jute fiber composites, J. Clean. Prod. 18 (4) (2010) 313–327, https://doi.org/10.1016/j.jclepro.2009.10.022.
[13] M. Khalfallah, B. Abbès, F. Abbès, Y.Q. Guo, V. Marcel, A. Duval, F. Vanfleteren, F. Rousseau, Innovative flax tapes reinforced Acrodur biocomposites: a new alternative for automotive applications, Mater. Des. 64 (2014) 116–126, https://doi.org/10.1016/j.matdes.2014.07.029.
[14] G. Koronis, A. Silva, M. Fontul, Green composites: a review of adequate materials for automotive applications, Compos. B Eng. 44 (1) (2013) 120–127, https://doi.org/10.1016/j.compositesb.2012.07.004.
[15] M. Habibi, L. Laperrière, G. Lebrun, L. Toubal, Combining short flax fiber mats and unidirectional flax yarns for composite applications: effect of short flax fibers on biaxial mechanical properties and damage behaviour, Compos. B Eng. 123 (2017) 165–178, https://doi.org/10.1016/j.compositesb.2017.05.023.
[16] L. Pil, F. Bensadoun, J. Pariset, I. Verpoest, Why are designers fascinated by flax and hemp fibre composites? Compos. Appl. Sci. Manuf. 83 (2016) 193–205, https://doi.org/10.1016/j.compositesa.2015.11.004.
[17] M. Habibi, G. Lebrun, L. Laperrière, Experimental characterization of short flax fiber mat composites: Tensile and flexural properties and damage analysis using acoustic emission, J. Mater. Sci. 52 (11) (2017) 6567–6580. https://doi:10.1007/s10853-017-0892-1.
[18] A. Jafari, H. Ashrafi, M. Bazli, T. Ozbakkaloglu, Effect of thermal cycles on mechanical response of pultruded glass fiber reinforced polymer profiles of different geometries, Compos. Struct. 223 (2019), 110959. https://doi:10.1016/j.compstruct.2019.110959.
[19] N. Iijima, H. Katogi, K. Takemura, Effect of thermal cycling after water absorption on flexural property of CFRP, Adv. Mater. Res. 1110 (2015) 19–22. https://doi:10.4028/www.scientific.net/amr.1110.19.
[20] S.Y. Park, W.J. Choi, C.H. Choi, H.S. Choi, An experimental study into aging unidirectional carbon fiber epoxy composite under thermal cycling and moisture absorption, Compos. Struct. 207 (2019) 81–92. https://doi:10.1016/j.compstruct.2018.08.069.
[21] Z.N. Azwa, B.F. Yousif, A.C. Manalo, W. Karunasena, A review on the degradability of polymeric composites based on natural fibres, Mater. Des. 47 (2013) 424–442. https://doi:10.1016/j.matdes.2012.11.025.
[22] S. Okubayashi, U. Griesser, T. Bechtold, A kinetic study of moisture sorption and desorption on lyocell fibers, Carbohydr. Polym. 58 (3) (2004) 293–299. https://doi:10.1016/j.carbpol.2004.07.004.
[23] M. Sit, C. Ray, Free vibration characteristics of glass and bamboo epoxy laminates under hygrothermal effect: a comparative approach, Compos. B Eng. 176 (2019), 107333. https://doi:10.1016/j.compositesb.2019.107333.
[24] C. Atas, A. Dogan, An experimental investigation on the repeated impact response of glass/epoxy composites subjected to thermal ageing, Compos. B Eng. 75 (2015) 127–134. https://doi:10.1016/j.compositesb.2015.01.032.
[25] T.H. Mokhothu, M.J. John, Review on hygroscopic aging of cellulose fibres and their biocomposites, Carbohydr. Polym. 131 (2015) 337–354. https://doi:10.1016/j.carbpol.2015.06.027.
[26] Z.E. Cherif, C. Poilâne, A. Vivet, B. Ben Doudou, J. Chen, About optimal architecture of plant fibre textile composite for mechanical and sorption properties, Compos. Struct. 140 (2016) 240–251. https://doi:10.1016/j.compstruct.2015.12.030.
[27] M. Assarar, D. Scida, A. El Mahi, C. Poilâne, R. Ayad, Influence of water ageing on mechanical properties and damage events of two reinforced composite materials: Flax–fibres and glass–fibres, Mater. Des. 32 (2) (2011) 788–795. https://doi:10.1016/j.matdes.2010.07.024.
[28] Z.E. Cherif, C. Poilâne, T. Falher, et al., Influence of textile treatment on mechanical and sorption properties of flax/epoxy composites, Polym. Compos. 34 (10) (2013) 1761–1773. https://doi:10.1002/pc.22580.
[29] E.H. Saidane, D. Scida, M. Assarar, R. Ayad, Assessment of 3D moisture diffusion parameters on flax/epoxy composites, Compos. Appl. Sci. Manuf. 80 (2016) 53–60. https://doi:10.1016/j.compositesa.2015.10.008.
[30] H. Dhakal, Z. Zhang, M. Richardson, Effect of water absorption on the mechanical properties of hemp fibre reinforced unsaturated polyester composites, Compos. Sci. Technol. 67 (7–8) (2007) 1674–1683. https://doi:10.1016/j.compscitech.2006.06.019.
[31] H.M. Akil, L.W. Cheng, Z.A. Mohd Ishak, A. Abu Bakar, M.A. Abd Rahman, Water absorption study on pultruded jute fibre reinforced unsaturated polyester composites, Compos. Sci. Technol. 69 (11–12) (2009) 1942–1948. https://doi:10.1016/j.compscitech.2009.04.014.
[32] P.A. Sreekumar, S.P. Thomas, J marc Saiter, K. Joseph, G. Unnikrishnan, S. Thomas, Effect of fiber surface modification on the mechanical and water absorption characteristics of sisal/polyester composites fabricated by resin transfer molding, Compos. Appl. Sci. Manuf. 40 (11) (2009) 1777–1784. https://doi:10.1016/j.compositesa.2009.08.013.
[33] A. Athijayamani, M. Thiruchitrambalam, U. Natarajan, B. Pazhanivel, Effect of moisture absorption on the mechanical properties of randomly oriented natural fibers/polyester hybrid composite, Mater Sci Eng A 517 (1–2) (2009) 344–353. https://doi:10.1016/j.msea.2009.04.027.
[34] A. Le Duigou, P. Davies, C. Baley, Exploring durability of interfaces in flax fibre/epoxy micro-composites, Compos. Appl. Sci. Manuf. 48 (2013) 121–128. https://doi:10.1016/j.compositesa.2013.01.010.
[35] K. Yorseng, S.M. Rangappa, H. Pulikkalparambil, et al., Accelerated weathering studies of kenaf/sisal fiber fabric reinforced fully biobased hybrid bioepoxy composites for semi-structural applications: Morphology, thermo-mechanical, water absorption behavior and surface hydrophobicity, Construct. Build. Mater. 235 (2020), 117464, https://doi.org/10.1016/j.conbuildmat.2019.117464.
[36] A.Q. Dayo, A.A. Babar, Q. Qin, et al., Effects of accelerated weathering on the mechanical properties of hemp fibre/polybenzoxazine based green composites, Compos. Appl. Sci. Manuf. 128 (2020), 105653. https://doi:10.1016/j.compositesa.2019.105653.
[37] A.S. Martín del Campo, J.R. Robledo-Ortíz, M. Arellano, M. Rabelero, A.A. Pérez-Fonseca, Accelerated weathering of polylactic acid/agave fiber biocomposites and the effect of fiber–matrix adhesion, J. Polym. Environ. 29 (3) (2020) 937–947, https://doi.org/10.1007/s10924-020-01936-z.
[38] S. Kumar, A. Saha, S. Bhowmik, Accelerated weathering effects on mechanical, thermal and viscoelastic properties of kenaf/pineapple biocomposite laminates for load bearing structural applications, J. Appl. Polym. Sci. 139 (2) (2021), 51465, https://doi.org/10.1002/app.51465.
[39] K. Senthilkumar, T. Ungtrakul, M. Chandrasekar, et al., Performance of sisal/hemp bio-based epoxy composites under accelerated weathering, J. Polym. Environ. 29 (2) (2020) 624–636. https://doi:10.1007/s10924-020-01904-7.
[40] H.N. Dhakal, C. Jiang, M. Sit, Z. Zhang, M. Khalfallah, E. Grossmann, Moisture absorption effects on the mechanical properties of sandwich biocomposites with cork core and flax/PLA face sheets, Molecules 26 (23) (2021) 7295. https://doi:10.3390/molecules26237295.
[41] British Standard Institute, Plastics – Determination of tensile properties – Part 2: Test conditions for moulding and extrusion plastics, BSI, London, 1996. BS EN ISO 527-2:1996.
[42] British Standard Institute, Plastics – Determination of flexural properties. BS EN ISO 178:2010+A1:2013, BSI, London, 2010.
[43] E. Muñoz, J.A. García-Manrique, Water absorption behaviour and its effect on the mechanical properties of flax fibre reinforced bioepoxy composites, Int J Polym Sci 2015 (2015) 1–10, https://doi.org/10.1155/2015/390275.
[44] A.C. Karmaker, A. Hoffmann, G. Hinrichsen, Influence of water uptake on the mechanical properties of jute fiber-reinforced polypropylene, J. Appl. Polym. Sci. 54 (12) (1994) 1803–1807. https://doi:10.1002/app.1994.070541203.